Molecular Crystals and Liquid Crystals Science and Technology. Section A. Molecular Crystals and Liquid Crystals
Publication details, including instructions for authors and subscription information:
http://www.tandfonline.com/loi/gmcl19

Liquid Crystalline Main Chain Polysiloxane Esters and their Monomers Part I: Synthesis of some di(ω-unsaturated esters) and their thermal behaviour

G. Koßmehl [a], B. Gerecke [a], N. Harmsen [a], F. Schröder [a] & H. M. Vieth [b]

[a] Institut für Organische Chemie der Freien Universität Berlin, Takustraße 3, 14195, Berlin, Germany

[b] Institut für Experimentalphysik der Freien Universität Berlin, Arnimallee 14, 14195, Berlin, Germany

Version of record first published: 24 Sep 2006.

To cite this article: G. Koßmehl , B. Gerecke , N. Harmsen , F. Schröder & H. M. Vieth (1995): Liquid Crystalline Main Chain Polysiloxane Esters and their Monomers Part I: Synthesis of some di(ω-unsaturated esters) and their thermal behaviour, Molecular Crystals and Liquid Crystals Science and Technology. Section A. Molecular Crystals and Liquid Crystals, 269:1, 39-53

To link to this article: http://dx.doi.org/10.1080/10587259508037320

Mol. Cryst. Liq. Cryst., 1995, Vol. 269, pp. 39–53
Reprints available directly from the publisher
Photocopying permitted by license only

Liquid Crystalline Main Chain Polysiloxane Esters and their Monomers

Part I: Synthesis of some di(ω-unsaturated esters) and their thermal behaviour.

G. KOßMEHL, B. GERECKE, N. HARMSEN and F. SCHRÖDER

Institut für Organische Chemie der Freien Universität Berlin, Takustraße 3, 14195 Berlin, Germany

H. M. VIETH

Institut für Experimentalphysik der Freien Universität Berlin, Arnimallee 14, 14195 Berlin, Germany

(Received February 10, 1994; in final form December 22, 1994)

As starting materials for liquid crystalline polyesters, a number of bis[4-(ω-alkenyloxybenzoyl)oxy]arenes (arising from the diols hydroquinone, 4,4'-biphenyldiol, 1,6-di(4-hydroxyphenyl)hexane, 2,7-fluorenediol and 2,7-fluorenonediol) have been synthesized and characterized by their elemental analyses, IR, ^{1}H NMR and MS. These esters exhibit liquid crystalline phases. The mainly nematic and in two cases also smectic phases have been studied by DSC and polarizing microscopy.

1. INTRODUCTION

Liquid crystalline main chain polymers (LCMCP) with polysiloxane ester units are of increasing interest for technical applications. The most frequently studied compounds are side chain polymers with polysiloxane units in the backbone. However, very little is known about the physical and liquid crystalline properties of polymers with polysiloxane ester units in the main chain. Thermotropic polyesters with linear mesogenic groups in the main chain based on hydroquinone ester units and highly flexible oligosiloxane spacers in the main chain were studied by Ringsdorf *et al.*[1]. These polymers were synthesized from O,O'-di[4-(ω-alkenyloxy)benzoyl]hydroquinone (with R = phenylene in the LCMCP formula) and H-terminated oligodimethylsiloxanes.

On the whole, it was found that with a reduction of the methylene spacer length (n) the range of the liquid crystalline phase is reduced.[2]

The aim of our work was to achieve a more detailed understanding of the relationship between molecular structure and macroscopic properties in liquid crystalline materials. For this reason we synthesized esters with different lengths of methylene

spacers and appropriate polymers with variable lengths of siloxane units [3,4] described in the following general formulas:

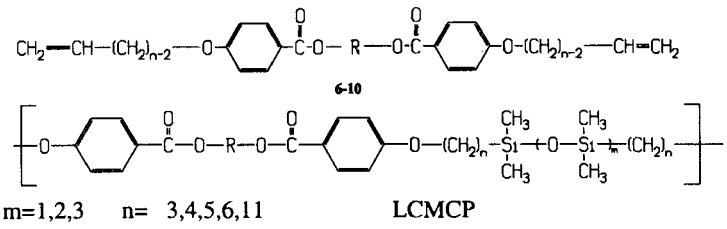

6-10

m=1,2,3 n= 3,4,5,6,11 LCMCP

SCHEME 1 General formulas of esters and polysiloxane esters.

We gave special care to the study on the influence of the ester structure on the phase behaviour. As diol components (with R), we used five different substances which are characterized by their symmetry and number of rings in the mesogenic group (Table 1).

In this paper we wish to present our work on the synthesis, structural characterization and thermal behaviour of the di(ω-unsaturated)esters **6–10**, which are starting materials for the synthesis of polymers. The general structure is given in Scheme 1. To begin we would like to discuss the liquid-crystalline behaviour of the esters **6–10**. As a rule, it is easier to study general relationships by observing rigid, low-molar-mass compounds, than main chain polymers. The latter are known for forming only relatively low ordered mesophases, so we will therefore first discuss the behaviour of the monomers to translate our information to the unknown main chain polymer systems.

Scheme 2 shows the synthetic route to the esters **6–10** arising from the diols 1,6-di(4-hydroxyphenyl)hexane (**1**), hydroquinone (**2**), 4,4′-biphenyldiol (**3**), 2,7-fluorenediol (**4**) and 2,7-fluorenonediol (**5**). The unsaturated group was introduced to the 4-ω-alkenyloxybenzoic acid by the reaction of allylbromide (n = 3), 4-bromobutene (n = 4), 5-bromopentene (n = 5), 6-bromohexene (n = 6) and 11-bromoundecene (n = 11).

2. SYNTHESIS AND CHARACTERIZATION

The monomers **6–10** were obtained by an esterification reaction of the diols **1–5** (see Table 1) with five ω-alkenyloxybenzoic acid chlorides in the presence of pyridine. The

TABLE 1

Characterization of the used diols

Diol	Symmetry	Mesogenic group
1,6-di(4-hydroxy-phenyl)hexane	flexible central chain	two ring system
hydroquinone	linear, rigid unit	three ring system
4,4′-biphenyldiol	linear, semiflexible unit	four ring system
2,7-fluorenediol	tilted, rigid unit	four ring system
2,7-fluorenonediol	tilted, rigid unit	four ring system

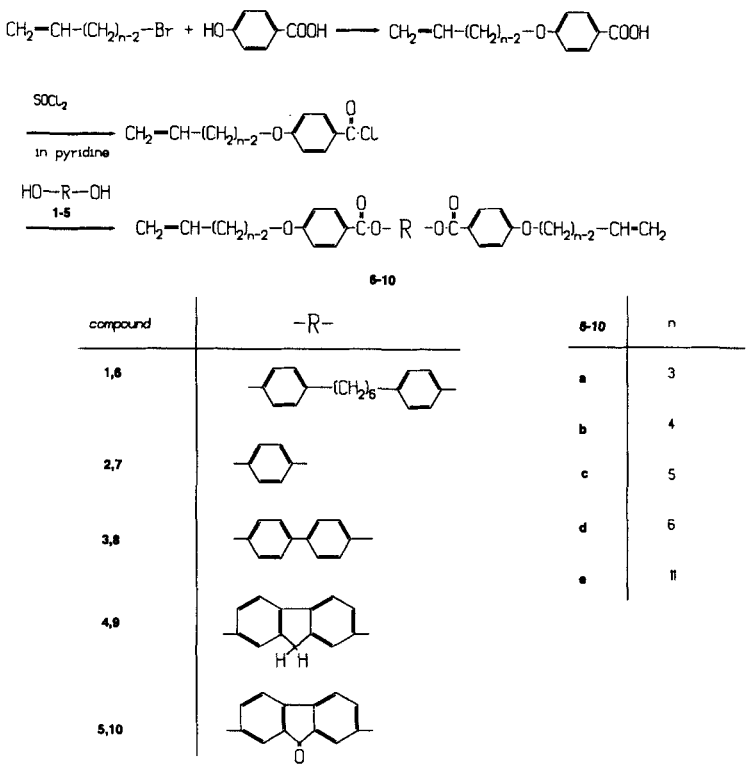

SCHEME 2 Synthetic route to the bis(ω-unsaturated) esters **6–10**.

synthesis is shown in Scheme 2. The structures of 25 synthesized, unsaturated esters were characterized by elemental analyses, IR, ^{1}H NMR and MS spectra (see Experimental Part and Table 3).

The thermal behaviour was studied by means of differential scanning calorimetry (DSC) and polarising microscopy. In addition to nematic phases, some of the esters also show smectic phases. For the related polymers we observed nematic textures.[6] The results of our studies on the di(α,ω-alkenyloxybenzoic acid)esters are summarised in Table 2.

3. RESULTS AND DISCUSSION

All the described unsaturated esters with different chain alkylene lengths formed from different diols show liquid crystalline behaviour which was studied by differential scanning calorimetry (DSC). The nature of the observed phase transitions was analysed in more detail by polarising microscopy.

In the majority of the materials, the second heating curve failed to reproduce the first one. Below the clearing point, an exothermic peak was observed at 250–280°C, probably resulting from a partly polymerisation reaction under cross-linking (this

TABLE 2

Phase transition temperatures of the liquid crystalline unsaturated esters

Compound	-R-	n	Phase transition temperatures in °C (transition enthalpies in J/g)
6a	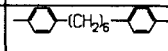	3	s/ 108(-45,1)/ N/ 187(-21,6 c))/ i i/ 166(13,7)/ N/ 56(24,2)/ s
6b	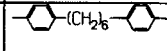	4	s/ 107(-61,7)/ N/ 171(-12,7 c))/ i i/ 169(9,54)/ N/ 77,2(37,3)/ s
6c	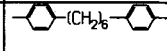	5	s/ 117(-120,9)/ N/ 149(-50,3 c))/ i i/ 147(53,9)/ N/ 78(125,8)/ s
6d	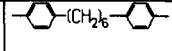	6	s/ 111(-142,1)/ N/ 137(-32,3 c))/ i i/ 134,3(35,2)/ N/ 79(131,9)/ s
7a	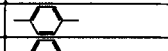	3	s/ 167/ N/ 243/ i a)
7b		4	s/148,5(-252,3)/ N/ 227,6(-14,8 c))/i
7c		5	s/ 132,7(-73,7)/ N/ 228,4(-4,52 c))/ i
7d		6	s/ 126,7(-182,6)/ N/ 193,3(-9,71 c))/ i
7e		11	s/ 103,4(-43,5)/ S_A/ 130,3(-4,35)/ N/ 168,3 (-3,03)/ i
8a	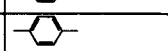	3	s/ 184,3(-233,8)/ N/ 277,6(-8,16 c))/ i b)
8b		4	s/ 149,7(-148,7)/ N/ 315,6(-14,8 c))/ i
8c		5	s/ 165,8(-210,2)/ N/ 352,9(-16,3 c))/ i
8d		6	s/150,9/ S_A/ 161(-66,9)/ N/ 324(-1,5 c))/ i
9a	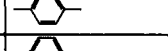	3	s/ 187(-195)/ N/ 273,8(-1,66 c))/ i
9b		4	s/ 154,2(-255)/ N/ 303(-1,88 c))/ i
9c		5	s/ 170,8(-114,7)/ N/ 320(-1,46 c))/ i
9d		6	s/ 139(-6,1)/ s/ 172,7(-141,4) / N/ 293 (-2 c))/i
10a	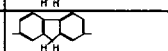	3	s/ 195,3(-57,8)/ N/ 283(-4,26 c))/ i
10b	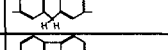	4	s/ 173(47,6)/ N/ 310(-3,4 c))/ i
10c	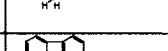	5	s/ 137(-17,4)/s/ 151,9(28,8)/ N/ 266 (-2,0 c))/i
10d	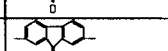	6	s/ 145(-62)/ s/ 154(-111,8)/ N/ 271 (-6,98 c))/i

[a] for comparison s 160 N 243 i (ref.5), [b] for comparison s 179 N 273 i (ref.5), s = solid, S_A = smectic A phase, N = nematic phase, i = isotropic melt, [c] during first heating

corresponds to the insolubility of the heated product) of several terminal ω-alkylene groups (Figure 1).

For this reason, all transition temperatures and enthalpies are based on the first heating curves. Further heating continuously decreased the transition peaks, due to a loss of movability of the mesogenic groups by cross-linking. The entropies of

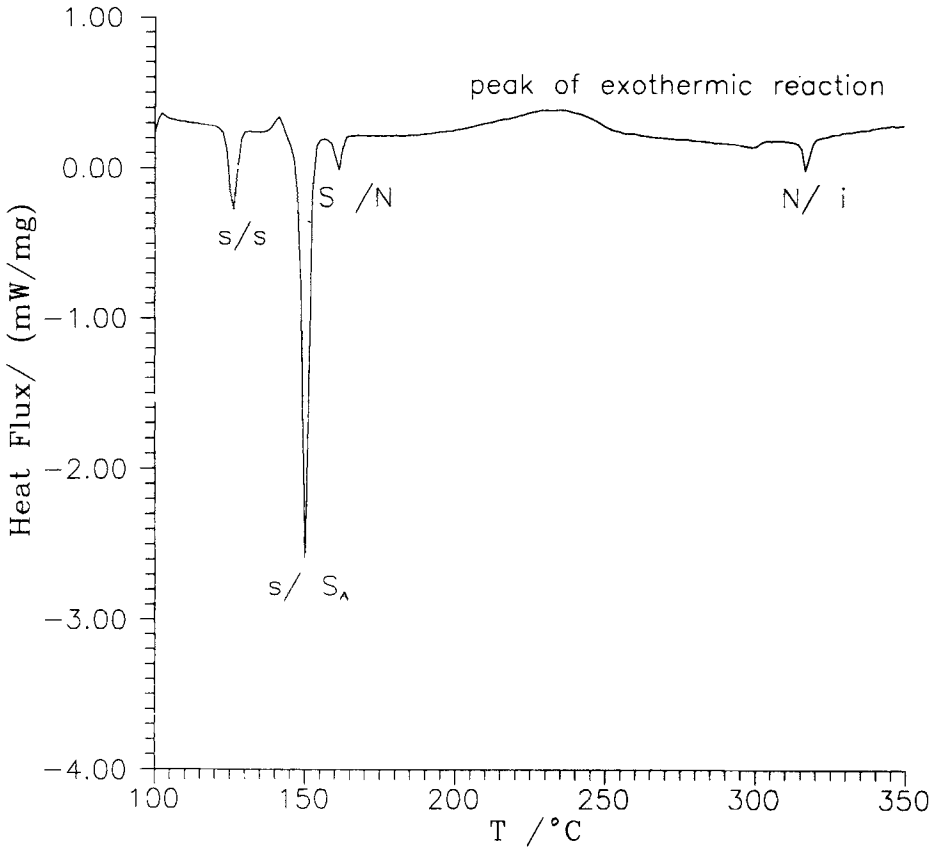

FIGURE 1 DSC-diagram of the diester **8d** (first heating; heating rate 10 K/min).

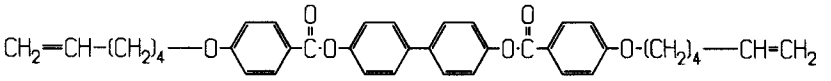

transitions higher than the exothermic peak must be locked upon with reservation, as the values in Table 2 are actually too low. In some cases it was necessary to determine the clearing point via polarising microscopy. In contrast the above described behaviour of our diesters with short alkylene chains, the diester with the longest alkylene chain length (**7e**, n = 11) is stable up to temperatures higher than the clearing point. In this case, identical first and second heating curves were observed.

The liquid crystalline behaviour of the di(ω-alkenyloxybenzoic acid)esters **6a–d** arising from 1,6-di(4-hydroxyphenyl)hexane as examples of a two ring system as mesogenic group was discussed in Figure 2. The data for these diesters confirm the theory that the clearing points decrease with increasing alkylene chain length, the melting points show no monotonous dependence on alkylene chain length, and the liquid crystalline ranges become narrower with an increasing length of the alkylene chain.

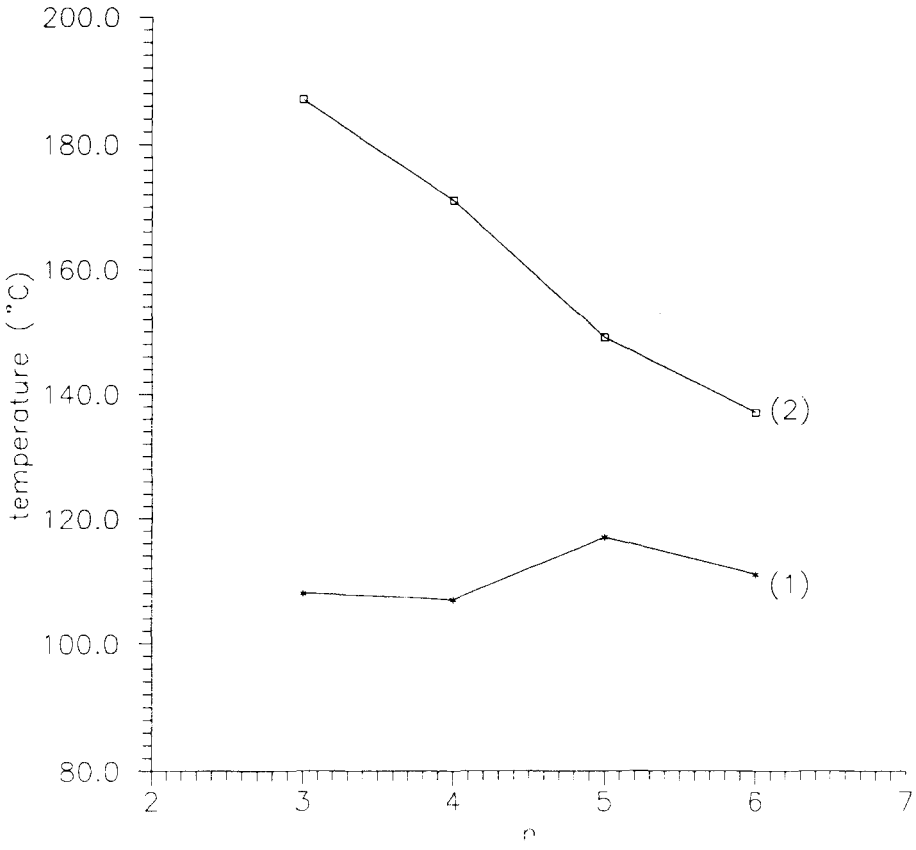

FIGURE 2 Influence of the alkylene chain length on the transition temperatures for the diesters **6a–d** (n = number of methylene groups) (1) melting points (s → N) (2) clearing points (N → i).

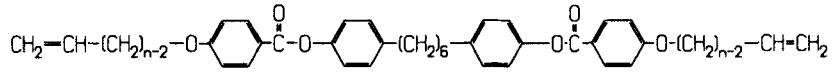

In Figure 3 the phase behaviour of the di(ω-alkenyloxybenzoic acid)esters **7a–e** with hydroquinone as diol is shown. The substances exhibit relatively low transition temperatures. As in Figure 2, the curves exhibit no monotonous behaviour, only for substance **7c**, a deviation from this general dependence was found, in which case the liquid crystalline phase was about 20K broader than expected (76K for **7a** and 79K for **7b**, respectively, compared to 96K for **7c**, and 67K for **7d**, 65K for **7e**). In addition to the nematic phase for the diester **7e** (n = 11) a smectic phase was also discovered. This low temperature phase gave regions of homeotropic and focal conic fan textures and was therefore assigned to a smectic A phase.

In order to study the change of the liquid crystalline ranges with respect to the size of the mesogenic group in Figure 4, we show the transition temperature dependence of differing four-ring systems for the di(ω-alkenyloxybenzoic acid)esters **8a–d** and **9a–d**.

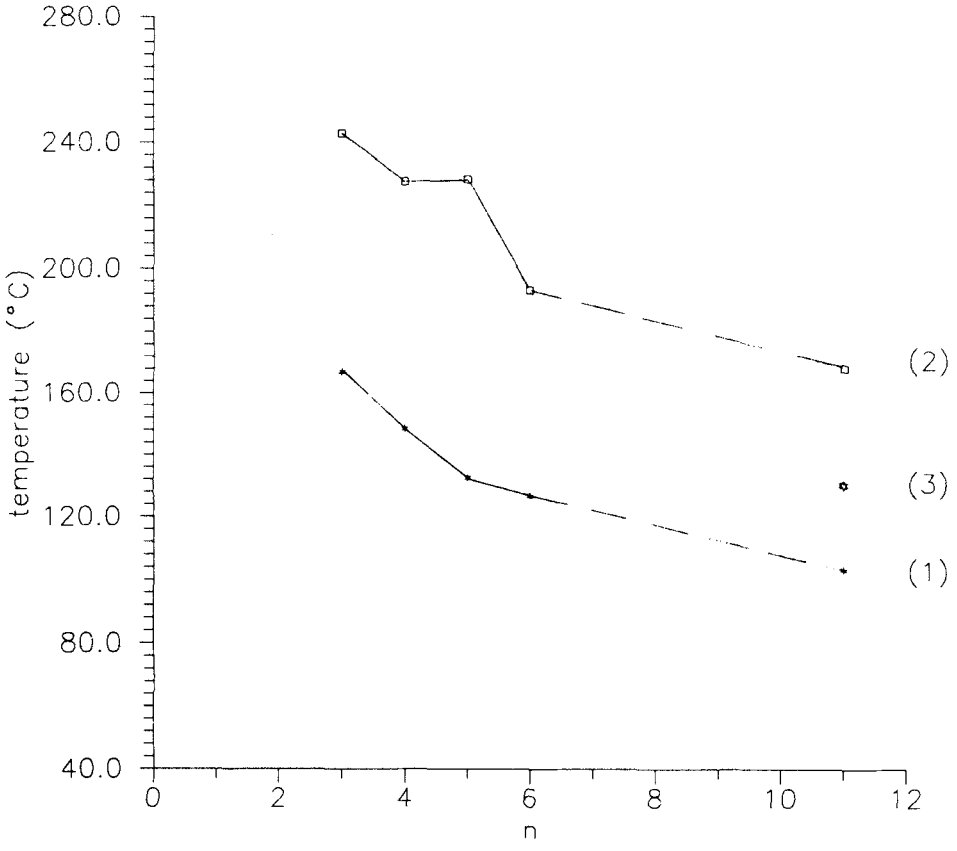

FIGURE 3 Influence of the alkylene chain length on the transition temperatures for the diesters **7a–e** (n = number of methylene groups). (1) melting points (s → N or S_A). (2) clearing points (N → i) (3) phase transition point (S_A → N).

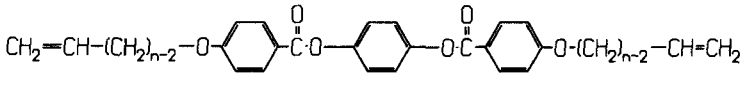

At first we found that generally the phase transitions occurred at higher temperatures than for the unsaturated diesters **6a–d** and **7a–e** containing two and three ring systems in the mesogenic groups. At second the temperature ranges were broader. Due to these high temperatures, thermal instability near the clearing point was observed.

The comparison of both series of the unsaturated diesters arising from 4,4′-biphenyldiol and 2,7-fluorenediol indicated, that the higher mobility of the 4,4′-biphenylene units increases the range of the liquid crystalline phase, but the effect is not particularly.

We found no significant differences between 2,7-fluorenediol and 2,7-fluorenonediol. In summary, typical liquid crystalline behaviour was observed for all described compounds. For comparison, we also prepared diesters using 4,4′-dihydroxybenzophenone as a diol component. Due to the "kinked" structure no LC phases were observed.

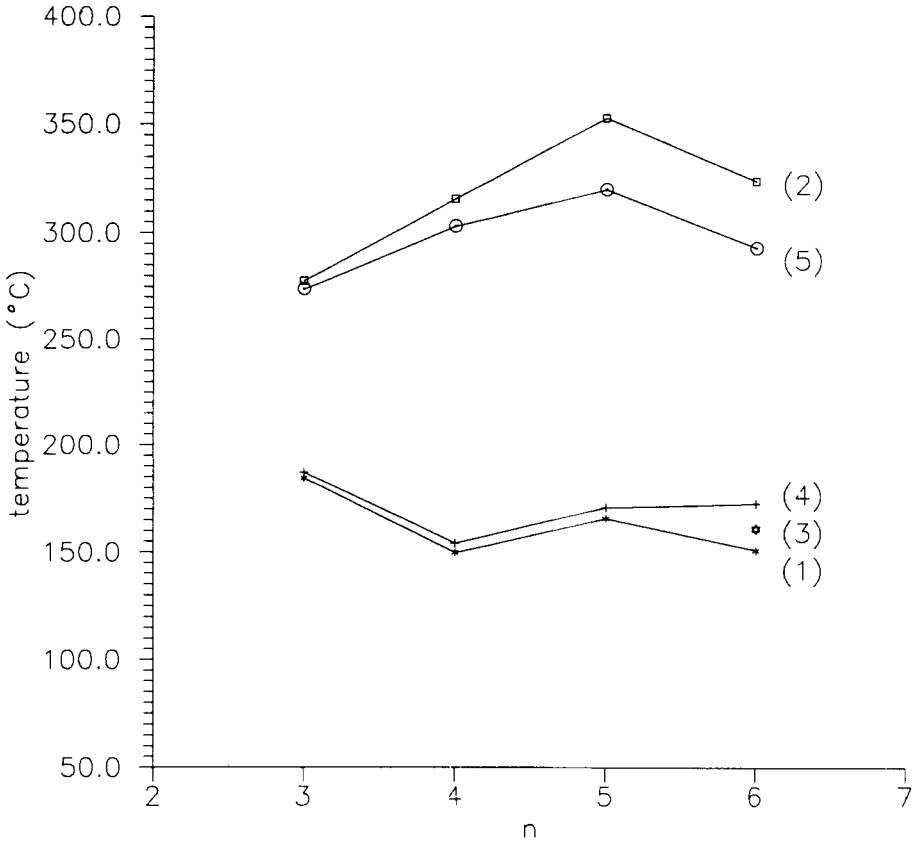

FIGURE 4 Comparison of the influence of the alkylene length on the transition temperature for the diesters **8a–d** and **9a–d**. (1) melting points **8a–d** (s → N). (2) clearing points **8a–d** (N → i). (3) phase transition point for **8d** (S_A → N). (4) melting points **9a–d** (s → N). (5) clearing points **9a–d** (N → i).

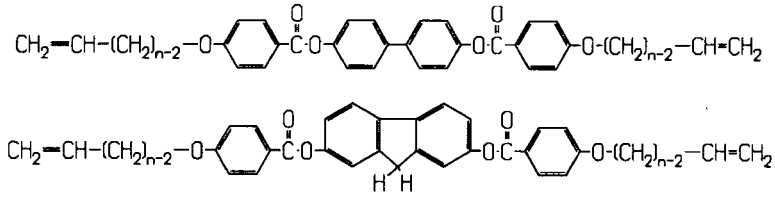

In a series of unsaturated diesters described above, only one substance (**8d**), showing additionally a smectic phase (S_A-phase see Figure 1, Figure 4 and Table 2) was found.

In order to categorize the liquid crystalline phases of all studied diesters, some textures[8] will be discussed in more detail. After melting, we observed non-classified (Ref. 8), nematic, "sand-like" textures, which changed within a small temperature range into typical nematic Schlieren textures (Figure 5a). With increasing temperature we find in a wide range black-white shadowy textures, which were difficult to see. For this

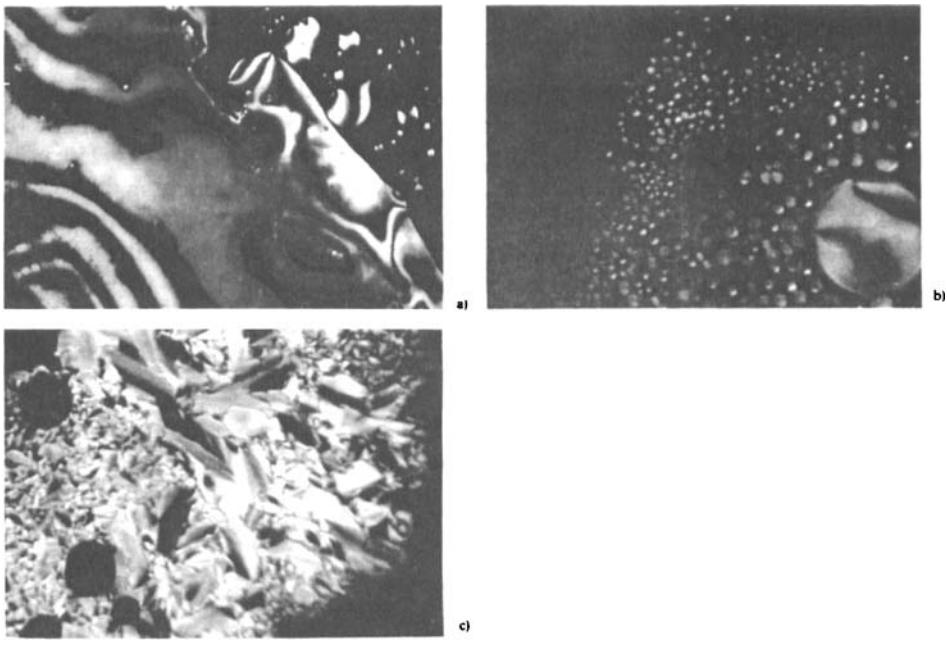

FIGURE 5a–c Microscopic picture of the textures. a) **6c**, 125°C, b) **6c**, 149°C, c) **7e**, 110°C. See Color Plate X.

reason it may be possible that some clearing points are higher than the given values. An important feature indicating the higher clearing point is given by the brightening of fast moving nematic droplets 5K below clearing temperature (Figure 5b).

Smectic phases can best be observed during cooling where nematic Schlieren textures change into fan-shaped textures as can be seen for compound **7e** (Figure 5c).

All compounds have nematic phases. Only two cases (**7e, 8d**) additionally showed smectic A phases. The even-odd effect for these compounds could not be found because the alkylene chains were not centralized in the molecule.

The aim of our work was to investigate the dependence of the transition temperature on the aromatic system and the alkylene spacer length.

In the substances **6a–d** where the central alkylene chain involves an uncoupled two ring system, a strong decrease of the clearing temperature with increasing alkylene chain length was observed. Due to the relatively constant melting points, the range of the LC-phases (80K (**6a**)–26K (**6d**)) decreased. By contrast, the esters **7a–e** with a rigid three ring system decreased the influence of the alkylene spacer length on the transition temperature. The LC-range is relatively constant (76K (**7a**)–65K (**7e**)). Both systems confirm the theory that with increasing movability resulting from an extension of the alkylene chain, the transition temperatures decreased.

If the mesogenic system becomes more rigid owing to the insertion of further aromatic units (4,4′-biphenyldiol or 2,7-fluorenediol), the LC-behaviour became increasingly determinated by the mesogenic system. As a result of the decreasing influence of the alkylene chains, increasing transition temperatures were found in spite of increasing alkylene chain length. However the transition temperatures of the rigid aromatic four ring systems were higher than those of the other substances.

4. EXPERIMENTAL PART

The structures of the new compounds were examined by IR and NMR spectroscopy, whereby the IR spectra were recorded with a Perkin Elmer 580-B spectrometer and the NMR spectra were performed on a Bruker-spectrometer WH 270/ AC 250 using tetramethylsilane as internal standard. A Zeiss microscope with a heating table (TMS 600) and polarising filter was used for texture observations. Thermal transformations were studied with a Netzsch DSC 200 at a scan rate of 10K/min under nitrogen. Peak maxima were taken as transition temperatures. Indium standards were used for thermal calibration and for calculation of transition enthalpies from peak areas.

General synthesis of the 4-(ω-alkenyloxy)benzoic acids (n = 3,4,5,6,11)
The 4-(ω-alkenyloxy)benzoic acids were synthesised from ω-alkenyl bromides and 4-hydroxy benzoic acid as reported previously.[7] The crude acids were recrystallized from ethanol or ethanol added water until precipitation.

General synthesis of the 4-di[(ω-alkenyloxy)benzoic acid]esters **6–10**
10 mmol of the previously mentioned acid were stirred with 20 mmol of thionyl chloride and two drops of N,N-dimethylformamide at room temperature. After 1h the excess of thionyl chloride was removed in vacuo. 5 mmol diol (**1–5**) were then dissolved in dry pyridine and added to the acid chloride under cooling. The mixture was stirred at room temperature for 3–4 h and then poured into 200 ml water. The precipitate was filtered off and dried. The crude product was purified by recrystallization from ethanol or acetone yielding colourless crystals. Yield, formula, molpeak and values of the elemental analyses data see Table 3.

1,6-Di[4-(4-allyloxybenzoyloxy)phenyl]hexane (**6a**)
From 1.78 g (10 mmol) 4-allyloxybenzoic acid and 1.35 g (5 mmol) **1**.
^{1}H NMR ($CDCl_3$) δ(ppm) = 8.12 (d, 4H, H_b); 7.20 (d, 4H, H_d); 7.05 (d, 4H, H_c); 6.92 (d, 4H, H_a); 6.04 (m, 2H, H_i); 5.40, 5.32 (2d, 4H, H_h); 4.6 (d, 4H, H_n); 2.55 (t, 4H, H_e); 1.65 (qui, 4H, H_f); 1.32 (m, 4H, H_g) (Characterization see Figure 6).
IR (KBr), ν(cm^{-1}) = 3100(w) ν(C—Harom); 2912,2830 (w) ν(C—H); 1731 (vs) ν(C=O); 1648 (sh) ν(C=Carom); 1604 (w), 1579 (w), 1511 (vs) ν(arom); 1256, 1074 (w) ν(O—Carom). These absorptions are also typical for the compounds **6b–d**.

1,6-Di{4-[4-(3-butenyloxy)benzoyloxy]phenyl}hexane (**6b**)
From 4-(3-butenyloxy)benzoic acid and **1**
^{1}H NMR ($CDCl_3$) δ(ppm) = 8.12 (d, 4H, H_b); 7.20 (d, 4H, H_d); 7.05 (d, 4H, H_c); 6.92 (d, 4H, H_a); 5.99 (m, 2H, H_i); 5.30, 5.20 (2d, 4H, H_h); 4.2 (t, 4H, H_n); 2.70–2.55 (m, 8H, H_e, H_k); 1.65 (qui, 4H, H_f); 1.32 (m, 4H, H_g) (Characterization see Figure 6.).

TABLE 3

Experimental analysis and characteristic data for compounds **6–10**

Compound	Yield (%)	Elemental Analysis				Mol. Peak[d]	Formula
		C(%) calc.	C(%) found	H(%) calc.	H(%) found		
6a[a]	58	77.27	77.23	6.48	6.39	590	$C_{38}H_{38}O_6$
6b[a]	53	77.64	77.37	6.84	6.72	618	$C_{40}H_{42}O_6$
6c[a]	55	77.99	77.51	7.17	7.03	646	$C_{42}H_{46}O_6$
6d[a]	61	78.31	78.26	7.47	7.43	674	$C_{44}H_{50}O_6$
7a[a]	66	72.55	71.63	5.51	4.97	430	$C_{28}H_{22}O_6$
7b[a]	45	73.35	73.05	5.72	5.60	458	$C_{26}H_{26}O_6$
7c[a]	59	74.05	74.28	6.21	6.31	486	$C_{28}H_{30}O_6$
7d[a]	70	74.68	74.59	6.66	6.51	514	$C_{30}H_{34}O_6$
7e[a]	75	77.03	77.00	8.31	8.22	654	$C_{42}H_{54}O_6$
8a[b]	55	75.87	75.60	5.17	5.22	506	$C_{32}H_{26}O_6$
8b[b]	43	76.39	76.34	5.66	5.58	534	$C_{34}H_{30}O_6$
8c[b]	57	76.85	76.78	6.09	5.89	562	$C_{36}H_{34}O_6$
8d[b]	60	77.27	77.18	6.48	6.25	590	$C_{38}H_{38}O_6$
9a[b]	57	76.43	76.35	5.05	5.00	518	$C_{33}H_{26}O_6$
9b[b]	39	76.91	76.75	5.53	5.34	546	$C_{35}H_{30}O_6$
9c[b]	59	77.32	77.18	5.97	6.00	574	$C_{37}H_{34}O_6$
9d[b]	60	77.71	77.45	6.36	6.28	602	$C_{39}H_{38}O_6$
10a[b]	65[c]	74.41	74.29	4.99	5.10	532	$C_{33}H_{24}O_7$
10b[b]	48[c]	74.98	74.56	5.04	4.98	560	$C_{35}H_{28}O_7$
10c[b]	68[c]	79.48	79.36	5.48	5.34	588	$C_{37}H_{32}O_7$
10d[b]	67[c]	79.94	79.67	5.89	5.76	616	$C_{39}H_{36}O_7$

[a] recrystallization from ethanol.
[b] solid material extraction performed in the Soxhlet apparatus.
[c] yellow crystals.
[d] from MS (EI/80 eV).

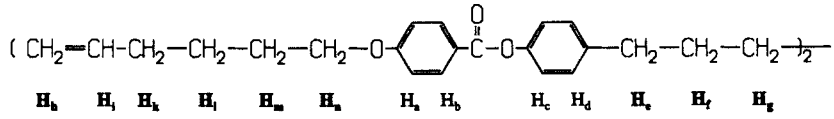

FIGURE 6 Characterization of the single groups of the ^{1}H NMR signals of **6a–d**.

1,6-Di{4-[4-(4-pentenyloxybenzoyloxy]phenyl}hexane (**6c**)
From 4-(4-pentenyloxy)benzoic acid and **1**.
^{1}H NMR ($CDCl_3$) δ(ppm) = 8.12 (d, 4H, H_b); 7.20 (d, 4H, H_d); 7.05 (d, 4H, H_c); 6.92 (d, 4H, H_a); 5.99 (m, 2H, H_i); 5.30, 5.20 (2d, 4H, H_h); 4.20 (t, 4H, H_n); 2.70 (t, 4H, H_e); 2.30 (qua, 4H, H_k); 1.95 (qui, 4H, H_l); 1.70 (qui, 4H, H_f); 1.32 (m, 4H, H_g) (Characterization see Figure 6.).

1,6-Di{4-[4-(5-hexenyloxybenzoyloxy]phenyl}hexane (**6d**)
From 4-(5-hexenyloxy)benzoic acid and **1**.
^{1}H NMR ($CDCl_3$) δ(ppm) = 8.12 (d, 4H, H_b); 7.20 (d, 4H, H_d); 7.05 (d, 4H, H_c); 6.92 (d, 4H, H_a); 5.90 (m, 2H, H_i); 5.20, 5.10 (2d, 4H, H_h); 4.10 (t, 4H, H_n); 2.68 (t, 4H, H_e); 2.20

(qua, 4H, H_k); 1.90 (qui, 4H, H_m); 1.70 (qui, 4H, H_f); 1.42 (m, 8H, H_g, H_l) (Characterization see Figure 6.).

O,O'-Di(4-allyloxybenzoyl)hydroquinone (**7a**)
From 4-allyloxybenzoic acid and **2**.
^{1}H NMR ($CDCl_3$) δ(ppm) = 8.2 (d, 4H, H_b); 7.25 (s, 4H, H_c); 6.96 (d, 4H, H_a); 6.1 (m, 2H, H_e); 5.3 (d, d, 4H, H_d); 4.6 (d, 4H, H_o) (Characterization see Figure 7).
IR (KBr), ν(cm^{-1}) = 3100(w) ν(C-Harom); 2912,2830 (w) ν(C—H); 1731 (vs) ν(C=O); 1648 (sh) ν(C = Carom); 1604 (w), 1579 (w), 1511 (vs) ν(arom); 1256, 1074 (w) ν(O-Carom). These absorption's are also typical for the compounds **7b-e**.

O,O'-Di[4-(3-butenyloxy)benzoyl]hydroquinone (**7b**)
From 4-(3-butenyloxy)benzoic acid and **2**.
^{1}H NMR ($CDCl_3$) δ(ppm) = 8.2 (d, 4H, H_b); 7.25 (s, 4H, H_c); 6.96 (d, 4H, H_a); 6.1 (m, 2H, H_e); 5.3 (d, d, 4H, H_d); 4.6 (t, 4H, H_o); 2.6 (d, t, 4H, H_f) (Characterization see Figure 7).

O,O'-Di[4-(4-pentenyloxy)benzoyl]hydroquinone (**7c**)
From 4-(4-pentenyloxy)benzoic acid and **2**.
^{1}H NMR ($CDCl_3$) δ(ppm) = 8.2 (d, 4H, H_b); 7.25 (s, 4H, H_c); 6.96 (d, 4H, H_a); 6.1 (m, 2H, H_e); 5.3 (d, d, 4H, H_d); 4.6 (t, 4H, H_o); 2.6 (d, t, 4H, H_f); 1.9 (t, t, 4H, H_g) (Characterization see Figure 7).

O,O'-Di[4-(5-hexenyloxy)benzoyl]hydroquinone (**7d**)
From 4-(5-hexenyloxy)benzoic acid and **2**.
^{1}H NMR ($CDCl_3$) δ(ppm) = 8.2 (d, 4H, H_b); 7.25 (s, 4H, H_c); 6.96 (d, 4H, H_a); 6.1 (m, 2H, H_e); 5.3 (d, d, 4H, H_d); 4.6 (t, 4H, H_o); 2.2 (d, t, 4H, H_f); 1.8 (t, t, 4H, H_h); 1.6 (t, t, 4H, H_g) (Characterization see Figure 7).

O,O'-Di[4-(10-undecenyloxy)benzoyl]hydroquinone (**7e**)
From 4-(10-undecenyloxy)benzoic acid and **2**.
^{1}H NMR ($CDCl_3$) δ(ppm) = 8.2 (d, 4H, H_b); 7.25 (s, 4H, H_c); 6.96 (d, 4H, H_a); 6.1 (m, 2H, H_e); 5.3 (d, d, 4H, H_d); 4.6 (t, 4H, H_i); 2.2 (d, t, 4H, H_f); 1.8 (m, 12H, H_g); 1.6 (t, t, 4H, H_h) (Characterization see Figure 7).

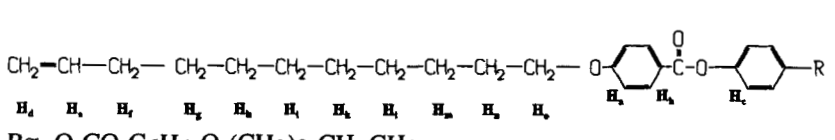

R≡ -O-CO-C_6H_4-O-$(CH_2)_9$-CH=CH_2

FIGURE 7 Characterization of the single groups of the ^{1}H NMR signals of **7a–e**.

4,4'-Di(4-allyloxybenzoyloxy)biphenyl (**8a**)
From 4-allyloxybenzoic acid and **3**.
^{1}H NMR ($CDCl_3$) δ(ppm) = 8.2 (d, 4H, H_b); 7.6 (d, 4H, H_d); 7.25 (d, 4H, H_c); 6.96 (d, 4H, H_a); 6.1 (m, 2H, H_f); 5.3 (d, d, 4H, H_e); 4.6 (d, 4H, H_k) (Characterization see Figure 8).
IR (KBr), ν(cm^{-1}) = 3100(w) ν(C-Harom); 2912,2830 (w) ν(C—H); 1727 (vs) ν(C=O); 1649 (sh) ν(C=Carom); 1606 (w), 1580 (w), 1509 (vs) ν(arom); 1256,1080 (w) ν(O-Carom). These absorption's are also typical for the compounds **8b–d**.

4,4'-Di[4-(3-butenyloxy)benzoyloxy]biphenyl (**8b**)
From 4-(3-butenyloxy)benzoic acid and **3**.
^{1}H NMR ($CDCl_3$) δ(ppm) = 8.2 (d, 4H, H_b); 7.6 (d, 4H, H_d); 7.25 (d, 4H, H_c); 6.96 (d, 4H, H_a); 6.1 (m, 2H, H_f); 5.3 (d, d, 4H, H_e); 4.6 (t, 4H, H_k); 2.6 (d, t, 4H, H_g) (Characterization see Figure 8).

4,4'-Di[4-(4-pentenyloxy)benzoyloxy]biphenyl (**8c**)
From 4-(4-pentenyloxy)benzoic acid and **3**.
^{1}H NMR ($CDCl_3$) δ(ppm) = 8.2 (d, 4H, H_b); 7.6 (d, 4H, H_d); 7.25 (d, 4H, H_c); 6.96 (d, 4H, H_a); 6.1 (m, 2H, H_f); 5.3 (d, d, 4H, H_e); 4.6 (t, 4H, H_k); 2.4 (d, t, 4H, H_g); 1.9 (t, t, 4H, H_h) (Characterization see Figure 8).

4,4'-Di[4-(5-hexenyloxy)benzoyloxy]biphenyl (**8d**)
From 4-(5-hexenyloxy)benzoic acid and **3**.
^{1}H NMR ($CDCl_3$) δ(ppm) = 8.2 (d, 4H, H_b); 7.6 (d, 4H, H_d); 7.25 (d, 4H, H_c); 6.96 (d, 4H, H_a); 6.1 (m, 2H, H_f); 5.3 (d, d, 4H, H_e); 4.6 (t, 4H, H_k); 2.4 (d, t, 4H, H_g); 1.9 (t, t, 4H, H_i); 1.6 (t, t, 4H, H_h) (Characterization see Figure 8).

2,7-Di(4-allyloxybenzoyloxy)fluorene (**9a**)
From 4-allyloxybenzoic acid and **4**.
^{1}H NMR ($CDCl_3$) δ(ppm) = 8.2 (d, 4H, H_b); 7.75 (d, 2H, H_e); 7.4 (s, 2H, H_c); 7.15 (d, 2H, H_d); 6.96 (d, 4H, H_b); 6.1 (m, 2H, H_h); 5.3 (d, d, 4H, H_g); 4.6 (t, 4H, H_m); 3.95 (s, 2H, H_f) (Characterization see Figure 9).
IR (KBr), ν(cm^{-1}) = 3077(w) ν(C—Harom); 2941, 2841 (w) ν(C—H); 1723 (vs) ν(C=O); 1649 (sh) ν(C=Carom); 1606 (w), 1580 (w), 1509 (vs) ν(arom); 1255, 1073 (w) ν(O-Carom); 1110 (s) ν(CH_2fluorene-9). These absorption's are also typical for the compounds **9b–d**.

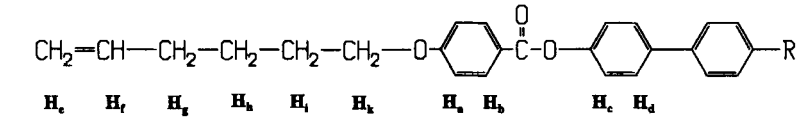

R≅ -O-CO-C_6H_4-O-CH_2-CH_2-CH_2-CH_2-CH=CH_2

FIGURE 8 Characterization of the single groups of the ^{1}H NMR signals **8a–d**.

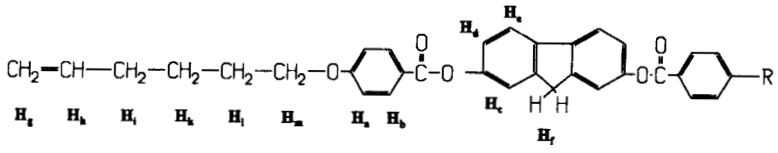

R≡ -O-CO-C_6H_4-O-CH_2-CH_2-CH_2-CH_2-CH=CH_2

FIGURE 9 Characterization of the single groups of the ^{1}H NMR signals **9a–d**.

2,7-Di[4-(3-butenyloxy)benzoyloxy]fluorene (**9b**)
From 4-(3-butenyloxy)benzoic acid and **4**.
^{1}H NMR ($CDCl_3$) δ(ppm) = 8.2 (d, 4H, H_b); 7.75 (d, 2H, H_e); 7.4 (s, 2H, H_c); 7.15 (d, 2H, H_d); 6.96 (d, 4H, H_b); 6.1 (m, 2H, H_h); 5.3 (d, d, 4H, H_g); 4.6 (t, 4H, H_m); 3.95 (s, 2H, H_f); 2.6 (d, t, 4H, H_i) (Characterization see Figure 9).

2,7-Di[4-(4-pentenyloxy)benzoyloxy]fluorene (**9c**)
From 4-(4-pentenyloxy)benzoic acid and **4**.
^{1}H NMR ($CDCl_3$) δ(ppm) = 8.2 (d, 4H, H_b); 7.75 (d, 2H, H_e); 7.4 (s, 2H, H_c); 7.15 (d, 2H, H_d); 6.96 (d, 4H, H_b); 6.1 (m, 2H, H_h); 5.3 (d, d, 4H, H_g); 4.2 (t, 4H, H_m); 3.95 (s, 2H, H_f); 2.4 (d, t, 4H, H_i); 2.1 (t, t, 4H, H_k) (Characterization see Figure 9).

2,7-Di[4-(5-hexenyloxy)benzoyloxy]fluorene (**9d**)
From 4-(5-hexenyloxy)benzoic acid and **4**.
^{1}H NMR ($CDCl_3$) δ(ppm) = 8.2 (d, 4H, H_b); 7.75 (d, 2H, H_e); 7.4 (s, 2H, H_c); 7.15 (d, 2H, H_d); 6.96 (d, 4H, H_b); 6.1 (m, 2H, H_h); 5.3 (d, d, 4H, H_g); 4.2 (t, 4H, H_m); 3.95 (s, 2H, H_f); 2.4 (d, t, 4H, H_i); 2.1 (t, t, 4H, H_l); 1.8 (t, t, 4H, H_k) (Characterization see Figure 9).

2,7-Di(3-allyloxybenzoyloxy)fluorenone (**10a**)
From 4-allyloxybenzoic acid and **5**.
^{1}H NMR ($CDCl_3$) δ(ppm) = 8.2 (d, 4H, H_b); 7.75 (d, 2H, H_e); 7.4 (s, 2H, H_c); 7.15 (d, 2H, H_d); 6.96 (d, 4H, H_b); 6.1 (m, 2H, H_g); 5.3 (d, d, 4H, H_f); 4.5 (t, 4H, H_n) (Characterization see Figure 10).

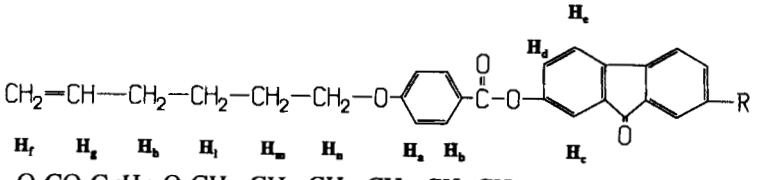

R≡ -O-CO-C_6H_4-O-CH_2-CH_2-CH_2-CH_2-CH=CH_2

FIGURE 10 Characterization of the single groups of the ^{1}H NMR signals **10a–d**.

IR (KBr), $\nu(cm^{-1})$ = 3077(w) ν(C-Harom); 2941, 2841 (w) ν(C—H); 1723 (vs) ν(C=O); 1710(vs) ν(C=O, fluorenone); 1649 (sh) ν(C=Carom); 1606 (w), 1580 (w), 1509 (vs) ν(arom); 1255,1073 (w) ν(O-Carom). These absorptions are also typical for the compounds **10b–d**.

2,7-Di[4-(3-butenyloxy)benzoyloxy] fluorenone (**10b**)
From 4-(3-butenyloxy)benzoic acid and **5**.
^{1}H NMR ($CDCl_3$) δ(ppm) = 8.2 (d, 4H, H_b); 7.75 (d, 2H, H_e); 7.4 (s, 2H, H_c); 7.15 (d, 2H, H_d); 6.96 (d, 4H, H_b); 6.1 (m, 2H, H_g); 5.3 (d, d, 4H, H_f); 4.2 (t, 4H, $H_i n$); 2.6 (d, t, 4H, H_h) (Characterization see Figure 10).

2,7-Di[4-(4-pentenyloxy)benzoyloxy] fluorenone (**10c**)
From 4-(4-pentenyloxy)benzoic acid and **5**.
^{1}H NMR ($CDCl_3$) δ(ppm) = 8.2 (d, 4H, H_b); 7.75 (d, 2H, H_e); 7.4 (s, 2H, H_c); 7.15 (d, 2H, H_d); 6.96 (d, 4H, H_b); 6.1 (m, 2H, H_g); 5.3 (d, d, 4H, H_f); 4.1 (t, 4H, H_n); 2.3 (d, t, 4H, H_h); 1.9 (t, t, 4H, H_i) (Characterization see Figure 10).

2,7-Di[4-(5-hexenyloxy)benzoyloxy] fluorenone (**10d**)
From 4-(5-hexenyloxy)benzoic acid and **5**.
^{1}H NMR ($CDCl_3$) δ(ppm) = 8.2 (d, 4H, H_b); 7.75 (d, 2H, H_e); 7.4 (s, 2H, H_c); 7.15 (d, 2H, H_d); 6.96 (d, 4H, H_b); 6.1 (m, 2H, H_g); 5.3 (d, d, 4H, H_f); 4.0 (t, 4H, H_l); 2.1 (d, t, 4H, H_h); 1.8 (t, t, 4H, H_k); 1.45 (t, t, 4H, H_i) (Characterization see Figure 10).

The financial support of the DFG is gratefully acknowledged.

References

1. C. Aguilera, H. Ringsdorf, A. Schneller, and R. Zentel, *IUPAC MACRO; Florence, Preprints* **3**, 306 (1980).
2. B.-W. Jo, J.-I. Jin, and R. W. Lenz, *Eur. Polym. J.* **18**, 233 (1982).
3. G. Koßmehl, B. Gerecke, N. Harmsen, and F. Schröder, *IUPAC, Dresden* (1993).
4. G. Koßmehl, B. Gerecke, N. Harmsen, and F. Schröder, to be published.
5. C. Aguilera, J. Bartulin, B. Hisgen, and H. Ringsdorf, *Makromol. Chem.* **184**, 253 (1983).
6. D. Demus, and L. Richter, *Textures of Liquid Crystals*, Weinheim (1978).
7. H. Ringsdorf, and A. Schneller, *Makromol. Chem., Rapid Comm.* **3**, 557 (1982).